Power System Resiliency During Wildfires Under Increasing Penetration of Electric Vehicles

Daniel L. Donaldson
Department of Electrical, Electronics, and Systems Engineering
University of Birmingham
Birmingham, United Kingdom
DLD818@bham.ac.uk

Manuel S. Alvarez-Alvarado
Department of Electrical, Electronics, and Systems Engineering
University of Birmingham
Birmingham, United Kingdom
manuel.alvarez.alvarado@ieee.org

Dilan Jayaweera
Department of Electrical, Electronics, and Systems Engineering
University of Birmingham
Birmingham, United Kingdom
d.jayaweera@bham.ac.uk

***Abstract*— Rising electric vehicle (EV) adoption is introducing new challenges to the operation and planning of the electric grid. Currently power system planners perform analysis to ensure adequate levels of reliability following contingencies such as loss of a substation. However, existing planning standards do not explicitly mandate studies of the redistribution of EV charging demand that would take place in the case of extreme events. Planning to serve the charging demand from EVs during extreme events is paramount to ensure the resiliency of the grid. This paper presents a novel framework for power system planners to reflect the impact of EV evacuations on grid resiliency during wildfire events. The method consists of resiliency analysis coupled with probabilistic models of load redistribution taking into account potential evacuation routes. A case study using the 2019 update to the IEEE 24 bus Reliability Test System (RTS) is performed to demonstrate the efficacy of the proposed strategy. The framework results in a more specific resiliency trapezoid that reflects a more realistic resiliency behaviour of the system.**

Keywords—Electric Vehicles, Generation, Natural Disasters, Power System Planning, Resilience

I. Introduction

Electric Vehicle (EV) adoption is accelerating with the global stock of electric passenger cars exceeding five million in 2018; an increase of 63% from the prior year [1]. This growth is anticipated to continue with the international energy agency forecasting nearly 150 million battery EVs worldwide by 2030 [1]. Effective management of EV can provide many benefits to the power grid in the form of increased flexibility, load shifting, and facilitation of decarbonization [2]. However, the rise of EVs has introduced new challenges for emergency planning, especially during evacuations due to natural disasters such as the recent wildfires in California [3]. Wildfires pose a significant risk, and in 2018 the state of California alone experienced 8,054 fires burning over 1.8 million acres [4]. The impact of resiliency planning for events such as earthquakes [5] and windstorms [6] has received much attention with authors in [6] proposing a resiliency trapezoid to reflect the phases a power system experiences during a natural disaster. However, the research related to resiliency planning with EV charging during natural disasters remains limited. One prior study is presented in [7] which highlights the complications with EV charging during a hurricane due to range limitations and lack of sufficient charging infrastructure. While this study provides insight into the need for charging infrastructure, it does not address the resiliency at the generation level.

The IEEE Task Force on the Definition and Quantification of Resilience recently defined resilience as [8]:

"*The ability to withstand and reduce the magnitude and/or duration of disruptive events, which includes the capability to anticipate, absorb, adapt to, and/or rapidly recover from such an event"*

In order to develop a resilient system in the face of increasing EV adoption, power system planners and operators need to account for adequate power to allow for vehicle charging during natural disasters. Unlike other loads, which remain geographically fixed, EV are mobile, and serve as a means of evacuation during a disaster. This mobile load can pose a problem if adequate generation capacity is not available to account for the generation, which may be forced offline during a fire. Currently, these issues may be limited due to the low penetration of EVs, but will grow in likelihood as EV demand increases significantly over the next decade.

The aim of this research is to enable grid planners and operators to better reflect the resiliency of the power system including EV charging demand during a wildfire. The contributions of this paper are: 1) Mathematical formulation to quantify the resiliency based on the total system generation during wildfire events; 2) Proposal of a novel model to reflect the impact of electric vehicle evacuation on system resilience; and 3) Refinement of the resiliency trapezoid presented in [6] to reflect wildfire behaviour. The efficacy of the proposed framework is demonstrated using the 2019 - IEEE Reliability Test System Grid Modernization Laboratory Consortium (RTS-GMLC) model. This model incorporates variable renewable generation as well as a modern portfolio of conventional generation, improving its applicability for real power systems.

The rest of the paper is structured as follows: Section II provides the resiliency framework; Section III describes the California case study and associated assumptions used to demonstrate the framework, Section IV discusses the results and major implications of the analysis, and Section V presents concluding remarks.

II. Power System Resiliency Framework

The impacts of wildfires can be geographically widespread. Therefore, the effect on the power system differs by hierarchy. Many components of the low voltage system may experience failure as a direct result of the fire. The transmission system components are typically more resilient to the effects of wildfires but may still experience outages. Finally, the effect on the generation system directly depends on the place where the fire occurs. As more generation is distributed, such as rooftop solar photovoltaics (PV), the exposure of the generation increases. While all three levels are important, this paper focuses on wildfire impacts at the generation level to assess the significance of increasing mobile loads (i.e. EV). Furthermore, transmission capacity limits are not considered in the study.

978-1-7281-2822-1/20/$31.00 ©2020 IEEE

Resiliency indices are measures used to quantify the vulnerability and performance of the system in the event that a wildfire occurs. At the generation level, the critical question is: *Is the total system generation sufficient to satisfy the demand during the emergency?* The proposed framework answers this question through the calculation of resiliency indices. To generate these indices a Markov chain of each generator and Monte Carlo simulation are adopted.

Authors in [6] developed a multi-phase resilience trapezoid to characterize the system's response to an event in three phases: I) Disturbance, II) Post-Disturbance degraded state, and III) Restorative state. This paper focuses on demonstrating the effect of EVs on Phase II.

A. Reliability Model-Based Markov Chain

The reliability model of a component is given by its availability A and unavailability U functions. Such functions can be obtained in terms of the probability density function of failure f, time to failure τ_f, probability density function of renewal g, repair time τ_r, time of normal operation t, and last repair time u. Mathematically, these are formulated as follows [9]:

$$A(t) = \int_0^{\tau_f} f(t)\,dt + \int_{\tau_f}^{\infty}\int_{\tau_f}^{\tau_r} f(t-u)g(u)\,du\,dt \quad (1)$$

$$U(t) = 1 - \int_0^{\tau_f} f(t)\,dt + \int_{\tau_f}^{\infty}\int_{\tau_f}^{\tau_r} f(t-u)g(u)\,du\,dt \quad (2)$$

As presented in (1) and (2), the solutions of the reliability model involve a complex mathematical process. Moreover, the accessibility information to the probability density function of failure and renewal are not frequently given by the manufacturers. To overcome the lack of this information, an alternate way to solve the models presented in (1) and (2) is by the employment of the Markov chain. The method consists of formulating a space state graph containing the possible operational states of each component, which are related through transition rate variables. In this paper, the components are modelled as an alternating renewable process between the normal operation and not in service states that are joined by the failure λ and repair μ rates, as presented in Fig. 1.

The solution of the Markov chain given in Fig. 1 has the form [10]:

$$A(t) = C_1 v_{11} e^{\chi_1 t} + C_2 v_{12} e^{\chi_2 t} \quad (3)$$

$$U(t) = C_1 v_{21} e^{\chi_1 t} + C_2 v_{22} e^{\chi_2 t} \quad (4)$$

where χ and $\boldsymbol{v}$ are the eigenvalues and eigenvectors of the stochastic matrix of transition states respectively; and C is a constant given by the initial conditions. The stochastic matrix of transition states **H** is an infinitesimal generator chain. Its diagonal terms h_{ii} are defined by the negative sum of the transitions rates that exit the state i, while the rest of the terms h_{ij} are defined by transition rates from i to j state [10]. Therefore, for the model presented in Fig. 1:

$$\mathbf{H} = \begin{bmatrix} -\lambda & \lambda \\ \mu & -\mu \end{bmatrix} \quad (5)$$

With the formulation given in (5) and knowing that the component is initially normally operating (initial condition: $A(0) = 1; U(0) = 0$), the terms χ, v, and C presented in (3) and (4) are derived. As a result, the availability and unavailability functions can be expressed as (6) and (7) respectively [9].

$$A(t) = \frac{\mu}{\mu+\lambda} + \frac{\lambda}{\lambda+\mu} e^{-(\lambda+\mu)t} \quad (6)$$

$$U(t) = \frac{\lambda}{\mu+\lambda} - \frac{\lambda}{\lambda+\mu} e^{-(\lambda+\mu)t} \quad (7)$$

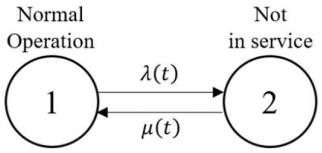

Fig. 1 Reliability model-based Markov chain

B. Resilience Indices Using Monte Carlo Simulation

The indices considered in this study are the loss of load expectation during natural disaster ($LOLEND$) given in hr/event duration, loss of load probability during the natural disaster ($LOLPND$) given in per unit, loss of energy expectation ($LOEEND$) given in MWh/event-duration, and system resiliency during natural disaster ($SRND$) given in percentage. For their determination, non-Sequential Monte Carlo simulation is used. The method starts by determining the operational state of each generator by producing random numbers for every one-hour time slot, during the duration of the natural disaster T_{ND}. The simulation considers the reliability model of each generator, to evaluate their operational state, such that if the generated number is greater than the unavailability (or less than the availability) then the generator's state is "not in service". Consequently, the total available generation capacity is obtained by merging the hourly operation of all individual generators [11]. The duration of the wildfire and the related case study assumptions are provided in Section III.

Monte Carlo simulation is executed for a total number of experiments M. In each experiment k, the time in which the demand not satisfied *TNS* and the energy not supplied ENS (both produced by the interruptions of the service and increment of the demand due to EV) are calculated. The *TNS* and ENS are obtained based on the available generation margin (see Fig. 2), that is, if the generation is not able to satisfy the demand (demand $>$ generation), then, the time and energy are recorded in *TNS* and ENS, repectively. Finally, the resiliency indices are calculated as given in (8) − (11).

$$LOLEND = \frac{1}{M}\sum_{k=1}^{M} TNS_k \quad (8)$$

$$LOLPND = \frac{LOLEND}{T_{ND}} 100\% \quad (9)$$

$$LOEEND = \frac{1}{M}\sum_{k=1}^{M} ENS_k \quad (10)$$

$$SRND = 1 \pm \frac{LOLEND}{T_{ND}} 100\% \quad (11)$$

The resiliency is analysed considering the geographical distribution of the power system components. The impact of the wildfire on the system is reflected by disconnecting all load and generation in the area of the wildfire. The EV load from the affected area is incorporated into the demand of neighbouring substations using the model presented in Section II. C. A flowchart of the proposed methodology is presented in Fig. 3

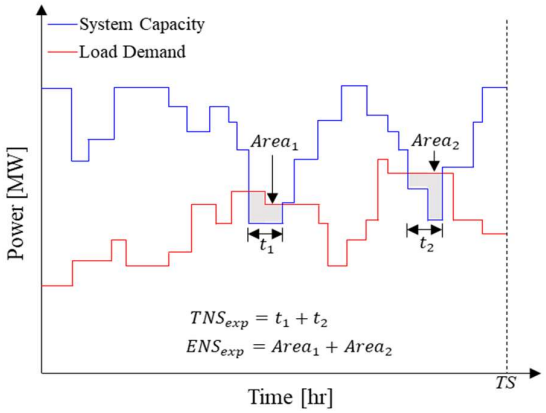

Fig. 2 Reserve margin identification

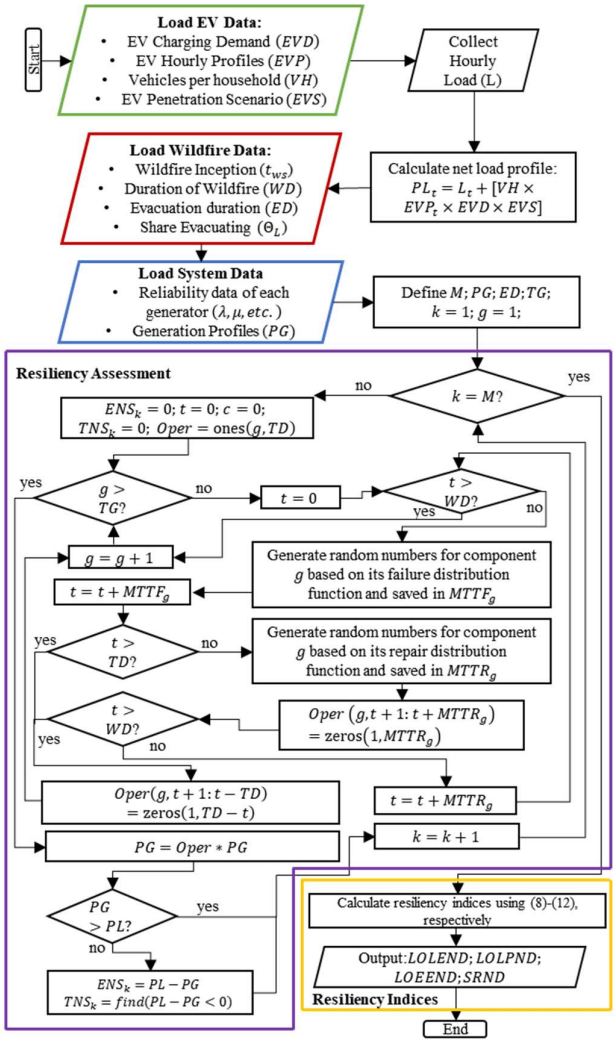

Fig. 3 Flowchart for resiliency assessment

C. EV Evacuation Model

The behaviour of residents in the Emergency Response Planning Area (ERPA) during a wildfire evacuation depends on a range of behavioural factors. Research has been conducted to better understand evacuation behaviour using data from actual natural disasters as described in [12]. Four critical factors must be identified to appropriately characterize the resiliency as depicted in Fig. 4: 1) The time for full power outage of the region (PS_t); 2) the Travel Time (tt); 3) Total Evacuation Time (WD); and 4) Wildfire Duration (WD).

The time at which the EVs arrive to their destination and begin charging again is a product of their final evacuation destination and the travel time to reach this destination. Distance plays a significant role in determining the choice of location for evacuees alongside other behavioural factors such as the size of the ensuing destination, availability of accommodation, and familiarity with the evacuation route [12]. In this paper, a proximity-based model is proposed to distribute the evacuated EVs from the wildfire area across the buses in the system. Mathematically, the EV allocation percentage at each bus (EVA_j) is calculated as

$$EVA_j = \begin{cases} C\ \Theta_L \dfrac{\frac{T}{d_j}}{\sum_{j=1}^{B} \frac{T}{d_j}} & \text{if } d_j \le R \\ 0 & \text{if } d_j > R \end{cases} \quad (12)$$

where C is the population of potential evacuating vehicles in the area; d is the distance to destination j; B is the total number of destinations; R is the range of the EV; and T is the sum of d across all possible destinations within the range. In addition, the proposed model considers the fact that not all residents will evacuate, as some households may be unaware of the disaster (and may ultimately be forced to shelter in place) and others choosing to stay and defend their homes. The term Θ_L represents the share of households who evacuate.

Once the EVA of each bus calculated as in (12), the travel time of vehicles to each of those locations is required. The travel time is calculated using household evacuation distribution (modelled by a Rayleigh distribution as noted by researchers in [12]) and drive time to reach the destination. Therefore,

$$tt_j = 1 - e^{-0.5\left(\frac{t_{ev}}{\beta}\right)^2} + \frac{d_j}{s} \quad (13)$$

where t_{ev} is the time after evacuation; β is the mode of the distribution function; s is the average speed of the car over the duration of the evacuation.

III. Case Study

For the analysis presented in this case study, MATLAB is used to perform the resiliency assessment, and python is used for the rest of the paper; numpy [13] and pandas [14] packages were used to perform the data preparation, geospatial analysis was done in geopandas [15] and visualization using matplotlib [16].

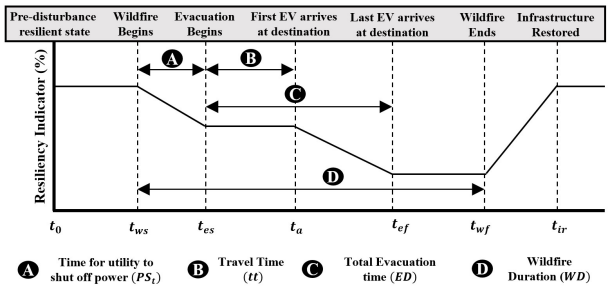

Fig. 4 Resiliency trapezoid for wildfire evacuation

A. IEEE 24 Bus Reliability Test System

In 2019, the RTS-GMLC model was proposed as an update to the IEEE Reliability Test System (RTS). The updated system introduces a modern generation mix and assigns a geographic location to the test system in the south-western United States [17]. For this paper, region 3 of the RTS-GMLC, located in California and consisting of 24 buses is used. A geographic location allows overlay of realistic wildfire hazard zones onto the system topology obtained from the California Public Utilities Commission (CPUC) [18]. The test system and wildfire risk zones are depicted in Fig. 5. While the geographical information given in the RTS-GMLC allows realistic wildfire threat zones and renewable energy profiles, it should be noted that the results of this analysis are not indicative of the real-world power system in this location. The generation capacity is summarized in Table I.

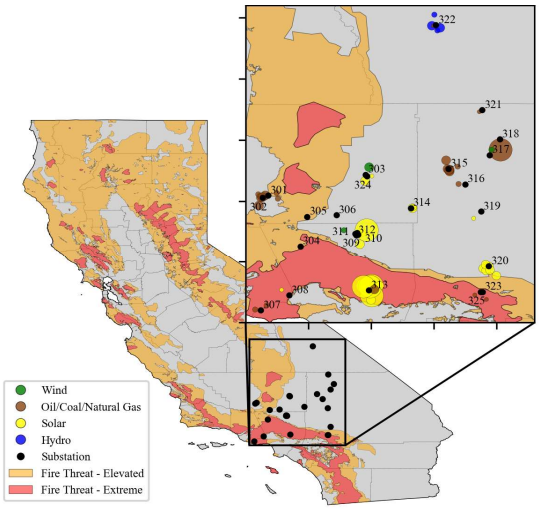

Fig. 5 Geographic Location with Wildfire Threat Zones

TABLE I. GENERATION MIX

Resource Type	Generation Capacity (MW)
Solar	2079.5
Wind	1794.4
Hydro	1000
Natural Gas	2380
Coal/Oil	295
Total	7548.9

TABLE II. LOAD ASSUMPTIONS

Assumption	Value
Total Area Peak Load	2,850 MW
Residential Load Share	50%
Individual Household Peak	4 kW
Number of Households	356,250

TABLE III. CALIFORNIA HOUSEHOLD VEHICLE OWNERSHIP [19]

Category	Estimate	Margin of Error
No Vehicle	939,034	+/-6,018
1 Vehicle	3,993,143	+/-12,465
2 Vehicle	4,838,980	+/-15,184
3+ Vehicles	3,194,278	+/-14,420
Total	12,965,435	+/-19,785

The load shape for region 3 of the RTS-GMLC is reflective of profiles of one of the balancing authorities in the area, as described in [17]. Further load assumptions are described in Table II. In addition, the number of vehicles in the region is calculated using demographic information from the U.S. Census Bureau for the state of California [19] and shown in Table III. Making the conservative assumption that no household has more than three vehicles, an average of 1.8 vehicles per household is obtained yielding ~640,000 vehicles in the area of study.

B. Electric Vehicle Penetration

To better assess the implications of the impact of EV penetration of wildfire evacuations, a base without EV (as reflected in RTS-GMLC) and ten additional scenarios were conducted at different EV penetration levels ranging from 10% to 100%. Level 2 charging at 3.3 kWh is assumed to reflect the limitations of some premises to a 20 amp feed as described in [20]. This is a conservative assumption of the potential impacts as vehicles could charge at substantially higher levels (19 kWh on a full EVSE level 2) and the charging levels continue to increase each year. The range of EVs is dependent upon the composition of the vehicle models present in the area of study and assumed to be 100 miles in this paper.

EV load shapes are based on the California Energy Commission's (CEC's) 2019 California IOU Electricity Load Shape Report [21] and are shown in Fig. 6. Consistent with this report, the breakdown in household charging load profiles is 68.9% single family residential (SF), 7.7% multifamily residential (MF), and 23.4% personal vehicle destination charging (PVDC). All households evacuating during the emergency are modelled using the personal vehicle destination charging profile, as these customers will no longer be able to rely on their own residential charging stations, but instead will be reliant upon finding charging stations in their destination.

C. Wildfire Assumptions

The Global Fire Atlas [22] uses data from 13.3 million individual fires from 2003-2016 to derive typical fire duration (in addition to other characteristics such as timing, location, daily expansion, spread, etc.). The mean duration for wildfires this part of North America weighted by fire size is 13.4 days [22]. The world average is 14.7 days. Therefore, for this analysis WD is set to be two weeks and the timeframe selected to be the two weeks of the summer peak.

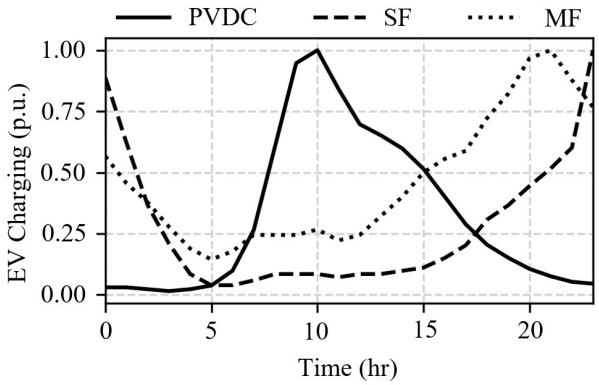

Fig. 6 Electric Vehicle Charging Profiles

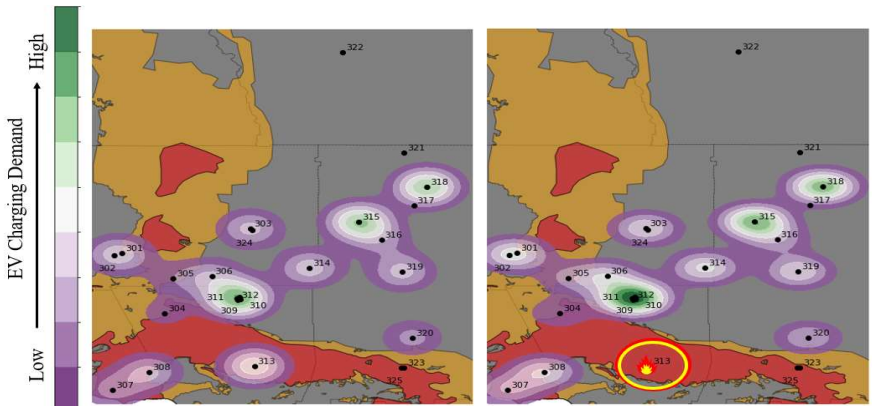

Fig. 7 Distribution of Electric Vehicle Charging Demand Before and After Wildfire

To calculate the necessary evacuation parameters, each of the load serving substations in network were considered and the distance between each is calculated. An average evacuation speed of 30 miles/hr is assumed and the range limit is 100 miles. Through evaluation of natural disasters with similar warning timeframes such as the volcanic eruption of Mt. St. Helens, or hurricanes which changed course, researchers identified 117 min to be a representative value of β for residents leaving from home [12] and is therefore used for this paper. A value of 89% is used for Θ_L to reflect the share of households who remain behind based on the sample mean of the survey of wildfire evacuation conducted in [23].

IV. Results and Discussion

In order to assess the power system resiliency during a wildfire, the first step is to determine the EV evacuation locations and how long it takes for households to travel there. The *EVA* was calculated at each bus using (12). The travel time to each location is obtained using (13). Fig. 7 shows the final allocation of EV during the wildfire, once all households have reached their ultimate destination.

The impact of wildfires can vary significantly based on the location, load and generation composition in the affected area, and the penetration and distribution of EVs throughout the system. For this study, it is assumed that the wildfire results in loss of the load and generation assets served from a single substation with the transmission lines remaining intact. Furthermore, as a uniform load composition is assumed at each bus, the base distribution of EVs prior to evacuation is directly proportional to the load at each bus.

When analysing the impact of the wildfire situation on the resiliency, it is apparent that the impacts will differ depending on the load and generation composition at each bus. The buses on the system can be grouped into two categories: Type I: Load exceeding generation; Type II: Generation exceeding load. Where load is in excess of the generation, during the wildfire the resiliency of the system improves due to the decline in load and the opposite occurs when the generation exceeds the load. A wildfire is simulated for one bus of each Type (I – Bus 308, and II – Bus 313) within the high fire risk area. The impact on resiliency can vary significantly based on the penetration of EVs. Fig. 8 shows an example of both bus types under varying penetration of EVs.

As can be seen in Fig. 8, the simulations for this case study validate the intuition that for buses without associated distributed or central generation, the resiliency of the system improves, even after consideration of EV evacuation. However, for Type II buses, the resiliency of the system is reduced during a wildfire and worsened further upon consideration of EV charging. This paper assumes an even penetration of EVs throughout the service territory. As the penetration the EV is heterogeneous, analysis of the impact of real EV distributions may lead to more pronounced impacts.

A more detailed evaluation of the impact of load composition, EV penetration, and evacuation charging impact can be seen in the numerical results for each resiliency index presented in Table IV. Each of the resiliency indices grow exponentially as more EV are present on the system. In this case study, a clear inflection point can be seen around 60% with the impact of EV evacuation contributing a 11% relative increase in the LOLPND over the wildfire case. The results also highlight the significant differences in system impact from evacuation at different levels of EV penetration.

Fig. 9 presents the empirical results from the case study and validates the refined model of power system resilience for a wildfire proposed in Fig. 4. When evaluating the resiliency of the system during a wildfire, it can be seen that the shape reflects two distinct resiliency levels: 1) During the fire but prior to evacuation and 2) Following evacuation. Planning for this second period is essential as it represents a degradation in reliability over the levels, which would be identified under the existing resiliency models. The refined model reflects an additional 0.5% decrease in SRND in comparison to the wildfire case which is 20% of the impact from the wildfire itself. Though the numbers will differ on a case by case basis, the fact that the EV evacuation impact was so large relative to the wildfire impact itself indicates the significance of modelling this effect during natural disaster planning.

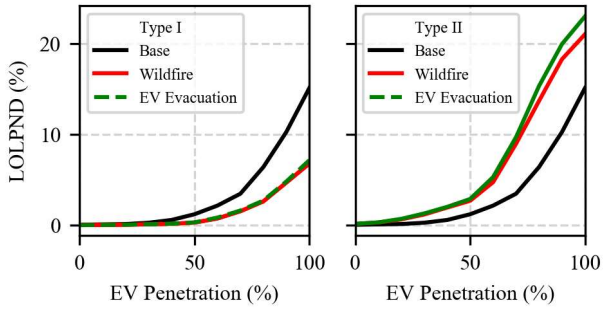

Fig. 8 Depiction of LOLPND for Type I and II buses following wildfire and subsequent addition of EV load.

TABLE IV. RESILIENCY INDICES FOR TWO BUSES

		Bus 308			Bus 313		
	EV Pen.%	Base	Wildfire	Evac	Base	Wildfire	Evac
LOEEND	0	14	3	3	14	62	62
	30	112	37	38	112	439	478
	60	1042	286	306	1042	2464	2694
	100	11359	4863	5083	11359	18927	20603
LOLEND	0	0.15	0.03	0.03	0.15	0.49	0.49
	30	0.89	0.34	0.35	0.89	3.98	4.33
	60	7.35	2.57	2.90	7.35	15.99	17.71
	100	50.70	22.76	23.96	50.70	70.59	76.78
LOLPND	0	0.05	0.01	0.01	0.05	0.15	0.15
	30	0.26	0.10	0.10	0.26	1.18	1.29
	60	2.19	0.76	0.86	2.19	4.76	5.27
	100	15.09	6.77	7.13	15.09	21.01	22.85
SRND	0	1.000	1.000	1.000	1.000	0.999	0.999
	30	0.997	0.999	0.999	0.997	0.988	0.987
	60	0.978	0.992	0.991	0.978	0.952	0.947
	100	0.849	0.932	0.929	0.849	0.790	0.771

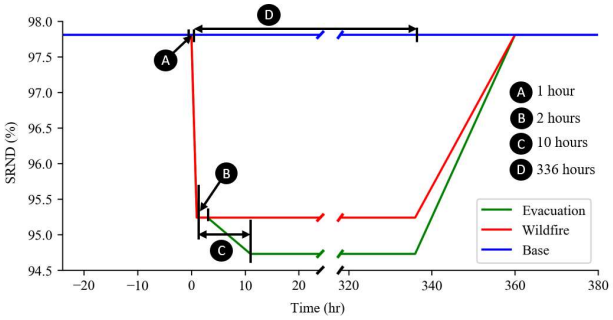

Fig. 9 Empirical Resiliency Trapezoid for a Wildfire at Bus 313 under 60% EV penetration

V. CONCLUSION

As more EVs appear on the system, power system operators should consider the ramifications of charging load during wildfire evacuations. The generation reserve margin during a natural disaster should account for EV charging demand and its geospatial dispersion to maintain resilience. The proposal of a novel EV evacuation impact model and more specific resiliency trapezoid (validated through the case study) allow for a better reflection of the true system resiliency during a wildfire. This paper shows that increasing EV penetration can cause an exponential increase in the resiliency indices. Therefore, the impact of EV evacuation on power systems will increase in importance as time progresses. Future works will consider the impact on power system security.

Utilities should also consider providing a means of charging to facilitate successful evacuation during a wildfire situation as the evacuation process may take several hours (~10 in the case study for this paper), and a portion of residents may remain behind. Therefore, utility public safety plans for wildfire events should include strategic consideration of EV charging.

ACKNOWLEDGMENTS

Manuel S. Alvarez-Alvarado would like to acknowledge the support of the Walter Valdano Raffo II program in Escuela Superior Politécnica del Litoral (ESPOL) and the Secretariat of Higher Education, Science, Technology and Innovation of the Republic of Ecuador (Senescyt).

REFERENCES

[1] "Global EV Outlook 2019 – Analysis - IEA." [Online]. Available: https://www.iea.org/reports/global-ev-outlook-2019#key-findings. [Accessed: 06-Feb-2020].

[2] P. J. Ramirez, D. Papadaskalopoulos, and G. Strbac, "Co-Optimization of Generation Expansion Planning and Electric Vehicles Flexibility," *IEEE Trans. Smart Grid*, vol. 7, no. 3, pp. 1609–1619, 2016.

[3] "Wildfires Forcing Electric Car Owners To Find New Ways To Power Up : NPR." [Online]. Available: https://www.npr.org/2019/11/08/777752175/with-blackouts-californias-electric-car-owners-are-finding-new-ways-to-charge-up?t=1580213208810. [Accessed: 28-Jan-2020].

[4] "National Interagency Coordination Center Wildland Fire Summary and Statistics," 2018.

[5] T. Lagos *et al.*, "Identifying Optimal Portfolios of Resilient Network Investments Against Natural Hazards, With Applications to Earthquakes," *IEEE Trans. Power Syst.*, vol. PP, no. c, pp. 1–1, 2019.

[6] M. Panteli, P. Mancarella, D. N. Trakas, E. Kyriakides, and N. D. Hatziargyriou, "Metrics and Quantification of Operational and Infrastructure Resilience in Power Systems," *IEEE Trans. Power Syst.*, vol. 32, no. 6, pp. 4732–4742, 2017.

[7] S. A. Adderly, D. Manukian, T. D. Sullivan, and M. Son, "Electric vehicles and natural disaster policy implications," *Energy Policy*, vol. 112, pp. 437–448, Jan. 2018.

[8] IEEE PES Industry Technical Support Task Force, "The Definition and Quantification of Resilience," PES-TR65, 2018.

[9] M. S. Alvarez-Alvarado and D. Jayaweera, "Reliability model for a Static Var Compensator," in *2017 IEEE Second Ecuador Technical Chapters Meeting (ETCM)*, 2017, pp. 1–6.

[10] M. S. Alvarez-Alvarado and D. Jayaweera, "Bathtub curve as a Markovian process to describe the reliability of repairable components," *IET Gener. Transm. Distrib.*, vol. 12, no. 21, pp. 5683–5689, 2018.

[11] M. S. Alvarez-Alvarado and D. Jayaweera, "Aging Reliability Model for Generation Adequacy," in *2018 IEEE International Conference on Probabilistic Methods Applied to Power Systems*, 2018, pp. 1–6.

[12] M. K. Lindell and C. S. Prater, "Critical behavioral assumptions in evacuation time estimate analysis for private vehicles: Examples from hurricane research and planning," *J. Urban Plan. Dev.*, vol. 133, no. 1, pp. 18–29, 2007.

[13] S. Van Der Walt, S. C. Colbert, and G. Varoquaux, "The NumPy array: A structure for efficient numerical computation," *Comput. Sci. Eng.*, 2011.

[14] W. McKinney, "Data Structures for Statistical Computing in Python. In Proceedings of the 9th Python in Science Conference," *Proc. 9th Python Sci. Conf.*, vol. 1697900, no. Scipy, pp. 50–59, 2010.

[15] K. Jordahl *et al.*, "geopandas/geopandas: v0.6.1." 12-Oct-2019.

[16] J. D. Hunter, "Matplotlib: A 2D graphics environment," *Comput. Sci. Eng.*, 2007.

[17] C. Barrows *et al.*, "The IEEE Reliability Test System: A Proposed 2019 Update," *IEEE Trans. Power Syst.*, vol. 35, no. 1, pp. 119–127, 2019.

[18] California Public Utilities Commission, "CPUC Fire Map." [Online]. Available: https://ia.cpuc.ca.gov/firemap/.

[19] United States Census Bureau, "American Community Survey 5-year Estimates Table DP04," *American FactFinder*, 2018. .

[20] B. Rubin, M. Chester, and J. Mankey, "Zero-Emission Vehicles in California : Community Readiness Guidebook," 2013.

[21] S. Baroiant, J. Barnes, D. Chapman, S. Keates, J. Phung, and I. . (ADM Associates, "California Investor-Owned Utility Electricity Load Shapes," 2019.

[22] N. Andela *et al.*, "The Global Fire Atlas of individual fire size, duration, speed, and direction," *Earth Syst. Sci. Data Discuss.*, no. August 2018, pp. 1–28, 2018.

[23] P. Mozumder, N. Raheem, J. Talberth, and R. P. Berrens, "Investigating intended evacuation from wildfires in the wildland-urban interface: Application of a bivariate probit model," *For. Policy Econ.*, vol. 10, no. 6, pp. 415–423, 2008.